JCARME
Journal of Computational and Applied Research in Mechanical Engineering
http://jcarme.srttu.edu
ISSN: 2228-7922
Vol. X, No. X, XXXX

Heat transfer characteristics of methane-air diffusion flames impinging normally on plane surfaces

SatyanandaTripathy[a], Manmatha K. Roul[b,*], Akshaya Ku. Rout[c]

[a]*School of Mechanical Engineering, KIIT University, Bhubaneswar, 751024, India*
[b]*Department of Mechanical Engineering., GITA, Bhubaneswar, 752054, India*
[c]*School of Mechanical Engineering, KIIT University, Bhubaneswar, 751024, India*

Article info:
Received: 04/08/2018
Accepted: 00/00/2019
Online: 00/00/2019

Keywords:
Diffusion flame;
heat transfer;
equivalence ratio;
Nusselt number;
Reynolds number

Abstract
Theoretical investigation of turbulent flame impinging normally on plane surfaces has been done to determine the average Nusselt number and the plate heat flux distribution as functions of jet Reynolds number, equivalence ratio (*ER*) and separation distance (*H/d*). The analysis is established on mathematical formulation of the governing equations for conservation of mass, momentum and energy. The turbulence phenomena is analyzed by the help of RNG *k-ε* turbulence model. The radiative heat transfer model has been designed by using Discrete Ordinates (*DO*) radiation model. It has been found that the heat flux gradually increases with the radial distance towards the plate centre and attains a maximum value at a location slightly away from stagnation point. The peak value in the local heat flux comes closer to the stagnation point when the height between the plates and the nozzle increases. Effects of variation of dimensionless separation distance on heat transfer characteristics have been investigated. It is observed that heat flux gradually improves when the value of H/d changes from 12 to 8 and decreases near the stagnation region with the further decrease in H/d from 8 to 4.

Nomenclature

C_p	Specific heat at constant pressure (kJ/kg K)
D	Mass diffusivity (m^2/s)
d	Diameter of burner (m)
H	Plate separation distance (m)
h	Enthalpy (kJ/kg)
K	Thermal conductivity (kW/m.K)
M	Molecular weight (kg/k.mol)
Nu	Nusselt number
p	Pressure (Pa)
q	Heat flux (kW/m^2)
Re	Reynolds number
R	Radius of plate (m)
r	Radius of burner (m)
T	Temperature (K)
U	Velocity (m/s)
Y	Mass fraction

Greek symbols

α	Thermal diffusivity (m^2/s)
ε	Turbulent dissipation rate (m^2/s^3)
γ	Stoichiometric air fuel ratio

[*]*Corresponding author*
Email address: mkroul@gmail.com

k	Turbulent kinetic energy (m^2/s^2)
μ_t	Turbulent viscosity (kg/m.s)
μ	Dynamic viscosity (kg/m.s)
ρ	Density (kg/m^3)
Subscripts	
f	Fuel
i	Inlet
o	Oxidizer
r	Radial direction
w	Wall
z	Axial direction

1. Introduction

The application of flame jets has been found in several industries to achieve better heat transfer coefficient and to produce high rates of heat transfer. Heating by flames in industrial furnaces is employed to increase heat flux and thereby reduce fuel consumption significantly. So it is used for various works such as internal combustion engines, cooling and combustion in gas turbine engines, heating of boiler, formation of glass in the industries, melting and surface treatment of metals. The lack of uniformity of heat flow near the stagnation point is a major drawback of the flame impingement heating process.

The heat transfer caused by the flame depends on the flame configuration, the temperature profile near the target plate, and the convection and radiation properties of components.

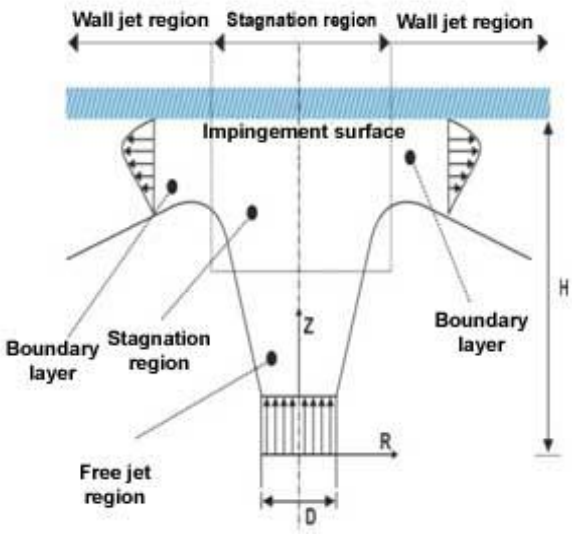

Fig. 1 Schematic diagram of flame impingement

The flame temperature depends on the structure of the impinging jet which includes wall jet region, free jet region and stagnation region as shown in fig. 1. Flame jet interaction with the ambient air at the outlet of the nozzle results in the growth of a non-uniform velocity profile in free jet region. In stagnation region the static pressure is more than ambient pressure as a result of which the pressure gradients in stagnation region suppresses the flow in axial direction as a result of which the flame turns in the radially outward direction. The wall jet region is free from mean pressure gradient.

Many researchers have investigated the flame impingement heat transfer experimentally and reported heat flux characteristics of methane-air flames impinging normally on target plates for various operating conditions. Baukal and Gebhart [1] reported that heat flux distribution on the plate surface due to flame impingement is non-uniform and peak value of heat flux was observed to have occurred not exactly at the stagnation point but a little away from it.

Boke et al. [2] investigate experimentally as well as theoretically the heat transfer phenomena using $k-\varepsilon$ turbulent model for modeling the turbulence phenomena in combustor. For modelling the radiative heat transfer they have used the discrete ordinates (DO) radiation model. Chander and Ray [3] observed that when the inner zone length is less as compared to the distance between target plate and nozzle, peak heat flux increases when Reynolds number increases. Majority of the studies using impinging flames for plane surfaces are carried out by Cornaro et al. [4] but surface curvature effect of the target plate have not been investigated at all. Dong et al. [5] proposed correlation for Nusselt number as a function of different geometrical and operational parameters. Hou and Ko [6] investigated heat transfer due to impinging flames on inclined plates and observed that the plate temperature and efficiency depend strongly on the plate separation distance.

Kuntikana and Prabhu [7] compared the heat transfer phenomena of premixed flame jets and isothermal air jets with variation of jet

Reynolds number to the target surface which is cooled from the opposite side. Agrawal et al. [8] studied the effect of impinging turbulent flames on inclined surfaces and found that when the oblique angle decreases the distribution of heat flux in lower part of the plate increases but in uphill part it is slightly dependent on of the oblique angle. The influence of convex curvature on heat transfer characteristic from an axi-symmetric jet is studied by Lee et al. [9] and found that at the stagnation point the Nusselt number increases with *d/D*.

Tripathy et al. [10] investigated theoretically diffusion as well as premixed flames impinging normally and obliquely on plane surfaces and found that the average Nusselt number over the plate increases when *Re* and *ER* increases and *H/d* decreases for both the flames. Mirmohammadi and Ommi [11] studied numerically the internal combustion diesel engines using *k-ε* turbulence models and observed that both linear and nonlinear *k-ε* turbulence models truly predicted flow direction inside the cylinder. Their results also demonstrated that nonlinear k-ε model predicted the energy amount of peak turbulent kinetics more than linear model. Ibrahim and Makinde [12] have studied the effect of radiation on MHD boundary layer through a porous vertical flat plate. Reddy et al. [13] investigated the effects of thermal radiation on the steady laminar flow of electrically conducting micropolar fluid past a stretching surface and observed that the skin-friction coefficient, heat and mass transfer rate decreases, and the gradient of angular velocity increases with an increase in porous medium inertia coefficient, inverse Darcy number and magnetic field parameter. Ibrahim and Suneetha [14] investigated analytically the free convection heat transfer through a non-homogeneous porous medium bounded by an infinite porous vertical plate in slip flow regime while considering thermal radiation, chemical reaction, the Soret number, and heat source. Prakash et al. [15] studied the influence of porous medium and diffusion on the flow of unsteady viscous fluid over a vertical permeable surface considering thermal radiation and first order chemical reaction.

Remie et al. [16] derived analytically the laminar flame impingement heat transfer and observed that the heal flux depends on the plate separation distance from the nozzle. Reddya and Sandeep [17] developed heat transfer characteristic of magneto-hydrodynamic free convective flow past a permeable rotating cone and a plate filled with gyrotactic microorganisms considering nonlinear thermal radiation and cross diffusion. Wei et al. [18] investigated experimentally impingement of laminar premixed biogas flame and found that with increase in the velocity of un burnt gas the heat flux as well as the total rate of heat transfer enhances significantly. Heat transfer properties of compressed natural gas were experimentally explored by Singh et al. [19] and presented the distribution of radial temperature of flames for various operating conditions and at axial heights.

Nayak et al. [20-21] investigated natural convection heat transfer from heated vertical pipes experimentally and developed correlations for Nusselt number and Rayleigh number. Sahoo et al. [22-23] studied numerically the natural convection heat transfer from vertical isothermal plate with protrusions and developed correlations to calculate the average Nusselt number as a function of fin spacing in the streamwise and spanwise directions, aspect ratio, and inclination of the fins. Gerdroodbary et al. [24] performed numerical simulation to predict the outcome of micro air jets on mixing of micro hydrogen jet in a supersonic flow. They observed that when the number of air jets are increased, the mixing performance of fuel jet increases significantly. Amini et al [25] investigated numerically the heat transfer taking swirling impinging jets and found that for L/D = 6 and 8, the rate of heat transfer of swirling jets were more than regular jets, and rate of heat transfer at higher Reynolds numbers increases due to higher rate of momentum transfer. Gerdroodbary et al [26-27] investigated numerically the effect of angle of shock waves on transverse hydrogen micro-

jets subjected to a supersonic crossflow focusing on mixing of hydrogen jet for high mach number with equivalence ratio of 0.5. Gerdroodbary et al [28] studied the thermal radiation effect on classical Jeffery–Hamel flow due to a point source or sink in convergent-divergent channels with stationary channel walls which is permitted to stretch or shrink. They observed that when the thermal radiation parameters are increased, the temperature profile also increases. Fallah et al. [29] performed numerical simulations to analyse the influence of micro air jets on the mixing of fuel in the cavity flame holder of the scramjet and observed that mixing of fuel in the cavity improves significantly by the injection of fuel in the middle of the vertical wall

2. Numerical solution

The physical model considered in the present work refers to a vertical flame jet impinging normally on a flat horizontal plate (Fig.1). Diffusion flames generated by circular and annular jet have been considered. The jet Reynolds number considered in this work refer to a steady, turbulent flame. RNG k-ε turbulent model is considered for analysis of turbulent flow in the flame.

The following assumptions have been made in this analysis:

1. The flow is turbulent but steady (based on time mean values of flow parameters).
2. The irreversible two step global reaction is considered for oxidation of methane.
3. The gas phase comprising air and products of combustion is assumed to obey the ideal gas laws.
4. Flow at the outlet of the nozzle is considered to be uniform.
5. The system is considered to be grey body with respect to radiation characteristics.

With all the above assumptions the governing equations are given by:

Conservation of Mass:

$$\nabla.(\rho\vec{v}) = 0 \qquad (1)$$

Conservation of Momentum:

$$\rho[\vec{v}\,.\nabla\vec{v}] = -\nabla p + \nabla.\left(\mu_{eff}\nabla\vec{v}\right) + \vec{F}_B \qquad (2)$$

where $\mu_{eff} = \mu + \mu_t = \mu + \rho c_\mu \frac{k^2}{\varepsilon}$

Here μ, μ_t and μ_{eff} are laminar viscosity, turbulent viscosity and effective viscosity respectively. $\vec{F}_B$ is the gravitational body force.

Turbulent Kinetic Energy:

$$\nabla.(\rho\vec{v}k) = \nabla.\left(\frac{\mu_t}{\sigma_k}\nabla k\right) + G_k - \rho\varepsilon \qquad (3)$$

Rate of Dissipation of Turbulent Kinetic Energy:

$$\nabla.(\rho\vec{v}\varepsilon) = \nabla.\left(\frac{\mu_t}{\sigma_\varepsilon}\nabla\varepsilon\right) + C_{1\varepsilon}\frac{\varepsilon}{k}G_k - \rho C_{2\varepsilon}\frac{\varepsilon^2}{k} \qquad (4)$$

where k, ε and G_k are the turbulent kinetic energy, rate of dissipation of turbulent kinetic energy and generation of turbulent kinetic energy respectively.

Conservation of Energy:

$$\nabla.(\rho\vec{v}h) = \nabla.\left(\rho\alpha_{eff}\nabla h\right) - \nabla.\vec{q}^r \qquad (5)$$

where $h = \sum_{k=1}^{N} Y_k\left[h_{f,k}^0 + \int_{T_{ref}}^{T} c_{p,k}\,dT\right]$

Here, h is the enthalpy of the mixture, h_f^0 is the enthalpy of formation, α_{eff} is the effective thermal diffusivity and Y_k is the mass fraction of component k.

Species Conservation:

$$\nabla.(\rho\vec{v}Y_k) = \nabla.\left(\rho D_{eff}\nabla Y\right) + S_k \qquad (6)$$

where D_{eff} and S_k represent effective mass diffusivity and source term for generation of k_{th} species respectively.

Mass diffusivity for two species A and B is calculated by the empirical formula [31]

$$D_{AB} = \frac{0.00266T^{3/2}}{PM_{AB}^{1/2}\sigma_{AB}^2\Omega_D} \qquad (7)$$

where M_A, M_B= Molecular weights of A and B

$$M_{AB} = 2\left[\left(\frac{1}{M_A}\right) + \left(\frac{1}{M_B}\right)\right]^{-1} \qquad (8)$$

P is the pressure in bar
T is the temperature in K
σ_{AB} = Characteristic length in Å = $\frac{\sigma_A+\sigma_B}{2}$

Chemical Kinetics:

The equations for oxidation of methane are given by:

$$CH_4 + 1.5O_2 = CO + 2H_2O$$

(9)

$$CO + 0.5O_2 = CO_2$$

(10)

The rate of reaction is given by Magnussen and Hjertager [31], as given below.

Arrhenius equation:

$$\dot{\omega}_{fk} = B(\rho)^{a+b} \frac{Y_f^a Y_o^b}{M_f^a M_o^b} exp\left(-\frac{E}{\bar{R}T}\right)$$

(11)

Magnussen and Hjertager equation:

$$\dot{\omega}_{fd} = A\frac{\rho}{M_f}\frac{\varepsilon}{k}\left[min\left(Y_f, \frac{Y_o}{\gamma}, \frac{cY_P}{1+\gamma}\right)\right]$$

(12)

where M and γ are molecular weight and stoichiometric ratio respectively.

Boundary conditions:

The flow field is assumed to be axi-symmetric and so, the computational domain is considered to be rectangular r - z plane, as shown in Fig. 2.

The boundary conditions considered for this analysis can be written in a cylindrical coordinate system as follows.

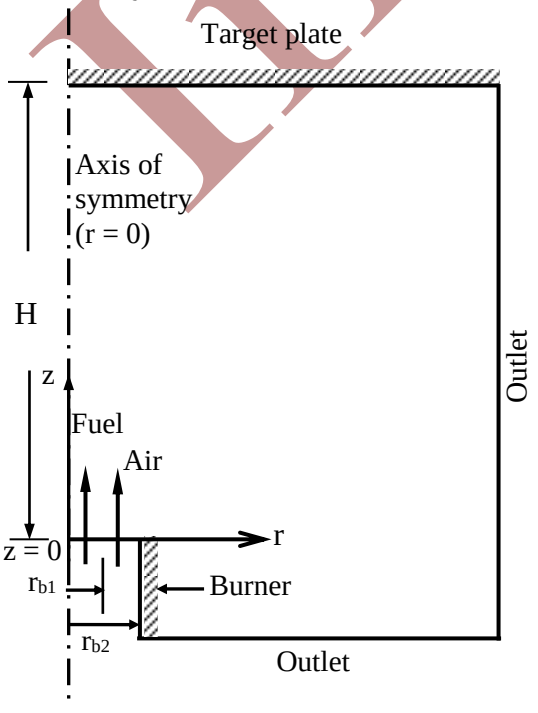

Fig. 2 Schematic diagram of computational domain

(i) At inlet (z = 0):

U_r = 0, U_z = U_{if}, T = T_i, Y_{CH4} = 1, Y_{O2} = 0, where ($0 \le r \le r_b$),
U_r = 0, U_z = U_{ia}, T = T_i, Y_{CH4} = 0, Y_{O2} = 0.23, Where ($r_{b1} \le r \le r_{b2}$)

where r_{b1} refers to the inner radius and r_{b2} refers to the outer radius of the nozzle.

(ii) At axis of symmetry (r = 0):

$$U_r = 0, \frac{\partial U_z}{\partial r} = \frac{\partial T}{\partial r} = \frac{\partial \rho}{\partial r} = \frac{\partial Y_k}{\partial r} = 0$$

(iii) At target plate (z = H):

No slip: U_r = 0,

No penetration: U_z = 0,

Isothermal: T = T_w

Impermeable: $\frac{\partial Y_k}{\partial z} = 0$

(iv) Outlet:

Radial direction: $\frac{\partial U_z}{\partial r} = \frac{\partial U_r}{\partial r} = \frac{\partial T}{\partial r} = \frac{\partial Y_k}{\partial r} = 0$

Axial direction: $\frac{\partial U_z}{\partial z} = \frac{\partial U_r}{\partial z} = \frac{\partial T}{\partial z} = \frac{\partial Y_k}{\partial z} = 0$

(v) Nozzle wall:

Adiabatic: $\left(\frac{\partial T}{\partial r}\right)_w = 0, or\ \dot{q}_w = 0$

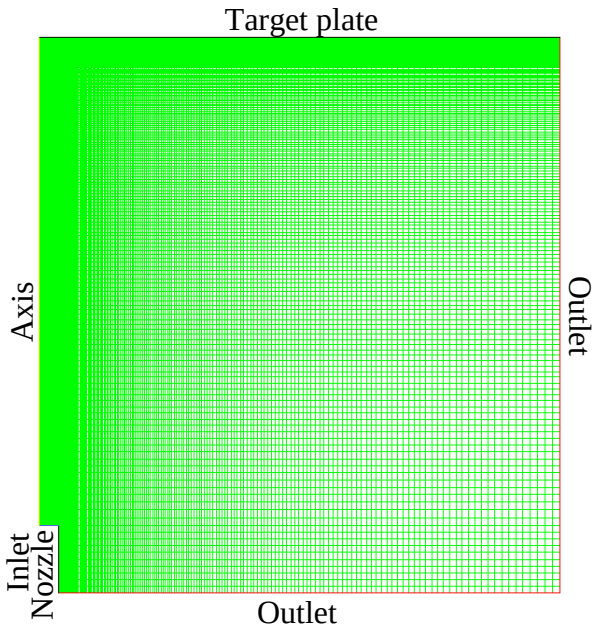

Fig. 3 Computational domain for H/d = 8

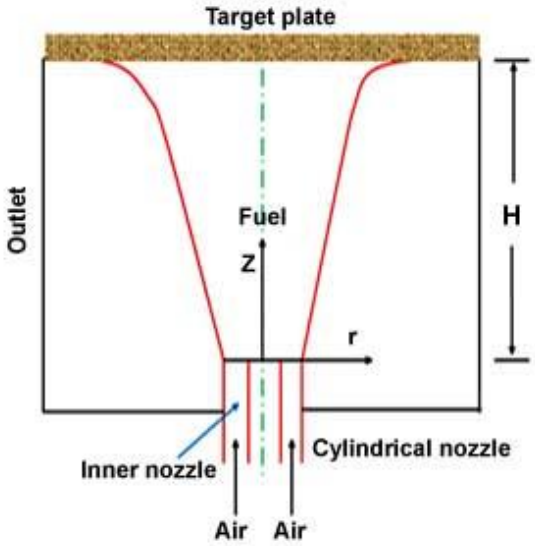

Fig. 4 Schematic diagram of diffusion flame impinging normally on plane surface

3. Numerical solution procedures

In the present work the conservation equations of mass, momentum, energy, turbulent kinetic energy, dissipation rate of turbulent kinetic energy, species conservation equations were solved by employing a fully time implicit finite volume technique using ANSYS Fluent software. SIMPLE algorithm was employed for pressure-velocity coupling. Second order upwind scheme was used for discretizing diffusion and advection terms. The convergence criteria for the residuals in all the discretized equations was set to 10^{-6}. Number of grids along radial and axial directions were taken as 150 (r) × 60 (z) to discretize for *H/d* = 4. For higher H/d ratios the number of grids along *z* direction was increased proportionately. For the numerical computations, methane was used as fuel and air was used as oxidizer. For diffusion flame the inner diameter of nozzle for the flow of fuel was taken as d_f = 4 mm and outer diameter of nozzle for the flow of air was taken as d_a = 12 mm. Temperature of fuel and air at inlet was considered to be 300K. The inlet velocities of air and fuel and separation distance of the target plate were varied to achieve the range of following dimensionless input parameters:

(i) Jet Reynolds number, $Re = \frac{\rho U_i d}{\mu}$: 2000, 6000, 8000, 10000, 15000

(ii) Equivalence ratio, $ER = \frac{(Y_a/Y_f)_s}{(Y_a/Y_f)_a}$: 0.8, 1.0, 1.2, 2.0

where subscript s stands for stoichiometric and a stands for actual air-fuel mixtures.

(iii) Ratio of distance of target plate and diameter of the nozzle, H/d: 4, 8, 12

For inlet velocity of fuel and air:
For fuel (methane) flow:
d = 0.004 m, at 300 K the kinematic viscosity = 17.28 * 10^{-6} m^2/s ,
Since, $Re = \frac{\rho U_i d}{\mu}$
For Re = 2000, U_{if} = 8.6 m/s and for Re = 15000, U_{if} = 64.8 m/s

So for fuel flow the velocity at inlet varies from 8.6 m/s to 64.8 m/s for the Jet Reynolds numbers varying from 2000 to 15000.

Similarly for air flow:
d = 0.008 m (hydraulic diameter), at 300 K the kinematic viscosity = 4.765 * 10^{-5} m^2/s,
Since, $Re = \frac{\rho U_i d}{\mu}$
For Re = 2000, U_{ia} = 11.91 m/s and for Re = 15000, U_{ia} = 89.34 m/s

So for air flow the velocity at inlet varies from 11.91 m/s to 89.34 m/s for the Jet Reynolds numbers varying from 2000 to 15000.
T_i is taken as 300 K.

4. Results and discussion

In this analysis an isothermal target plate of specified temperature is considered. The theoretical predictions of this model for the case of premixed flame is compared with the experimental data of Vander Meer [32] as illustrated in Table 1. The theoretical results of the present model matches closely with the experimental data.

For the grid independence test several numerical experiments were conducted to determine the optimum number of grids along radial and axial directions.

Table 1 Comparison of present theoretical predictions with experimental data [32]

Fixed input parameters	Variable parameters for both experimental (32) and present model	Nu (at stagnation point)	
Fuel: Methane Premixed flame *ER* = 1.0 *Re* = 4226	H/d	Experimental results [32]	Theoretical predictions by present model
	2	68.25	60.20
	4	112.10	103.25
	6	116.50	108.40
	8	107.90	97.30

Table 2 shows the variation of average Nusselt number with number of cells for various values of *H/d* for *Re* = 6000.

Table 2 Grid independence test.

Sl. No.	H/d = 4		H/d = 8		H/d = 12	
	No. of grids	Nu	No. of grids	Nu	No. of grids	Nu
1	3000	175.20	12000	162.75	27000	126.35
2	4800	278.32	19500	257.65	43200	199.45
3	7000	267.6	26400	246.32	63000	188.25
4	9000	260.45	36000	241.25	81000	183.68
5	12600	259.66	56250	240.65	113400	182.92
6	20000	258.95	80000	240.02	140000	182.25

Fig. 5 depicts the dependence of Nusselt Number on grid size for various values of *H/d*.

It is evident from Table 2 and Fig. 5 that for H/d = 4, as number of grids in the domain increases from 3000 to 9000, average Nusselt number changes from 175.20 to 260.45. Further increase in number of grids up to 20000 has negligible effect on Nusselt number. Similarly for H/d = 8, as the number of grids in the domain increases from 12000 to 36000, average Nusselt number changes from 162.75 to 241.25. Further increase in number of grids up to 80000 has negligible effect on the average Nusselt number. And for H/d = 12, as the number of cells in the domain increases from 27000 to 81000, average Nusselt number changes from 126.35 to 183.68. Further increase in number of grids up to 140000 has almost no effect or negligible effect on the average Nusselt number.

The fig. 6 illustrates the distribution of heat flux at the surface of the plate for various values of H/d for *ER*=1 (based on flow of air through annular nozzle), and fuel jet Reynolds number of 6000. The qualitative trends of heat flux distributions are almost the same as that in case of premixed flame (Tripathy et al. [10]).

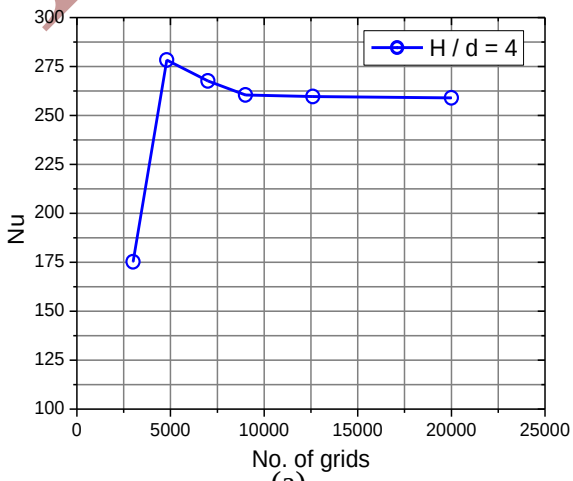

(a)

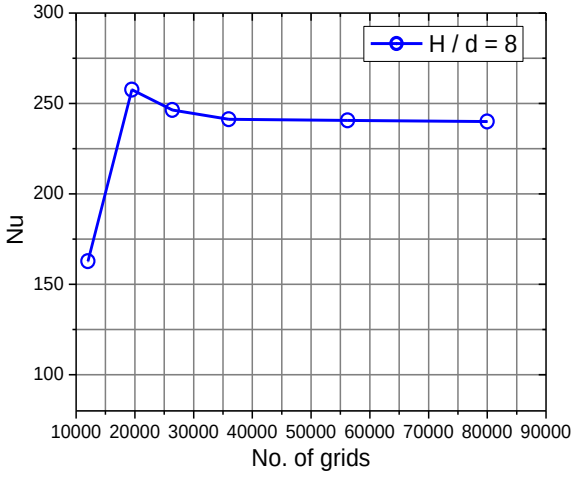

(b)

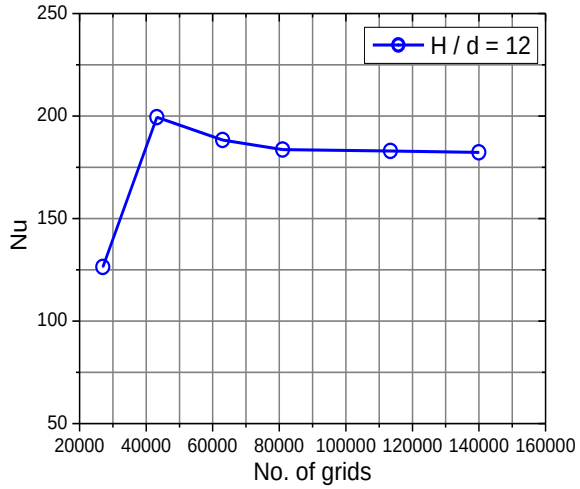

(c)

Fig. 5 Average Nusselt number as a function of grid size for (a) *H/d* =4, (b) *H/d* =8 and (c) *H/d* = 12

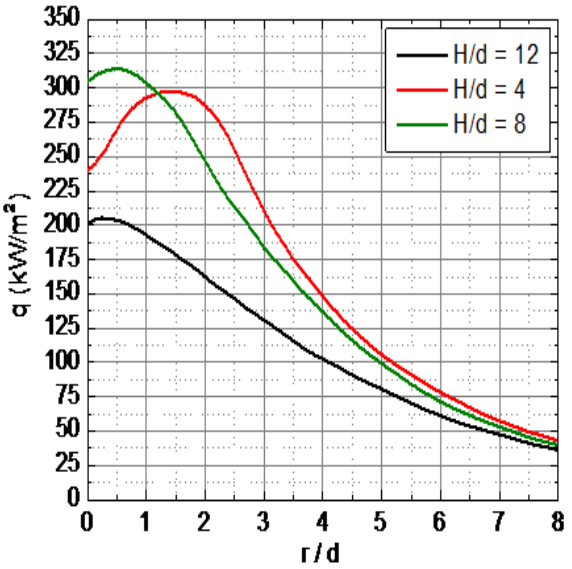

Fig. 6 Heat flux for various values of plate separation distance (*Re* = 6000, *ER* = 1)

The main differences in the results with those of premixed flames are that the plate heat flux at any radial location for a given value of H/d is higher in diffusion flames. Heat flux increases significantly with a relatively flat distribution at the peak point.

Similarly, the variation of heat flux at the plate surface for various values of *H/d* for *ER* = 1, and fuel jet *Re* = 10000 is given in fig. 7.

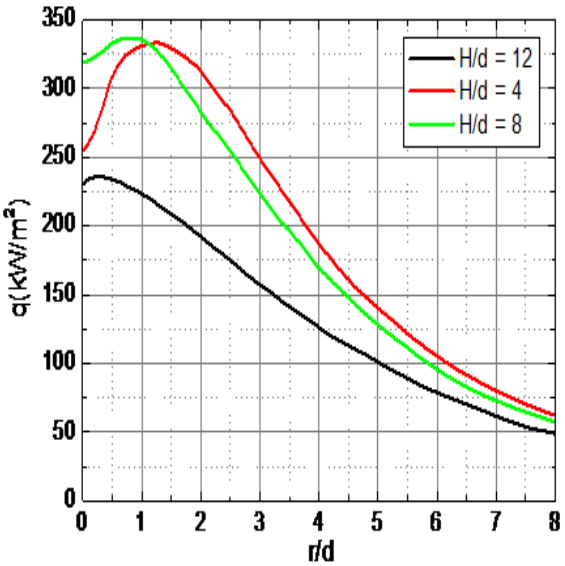

Fig. 7 Heat flux distributions for various plate separation distance (Re = 10000 and ER = 1)

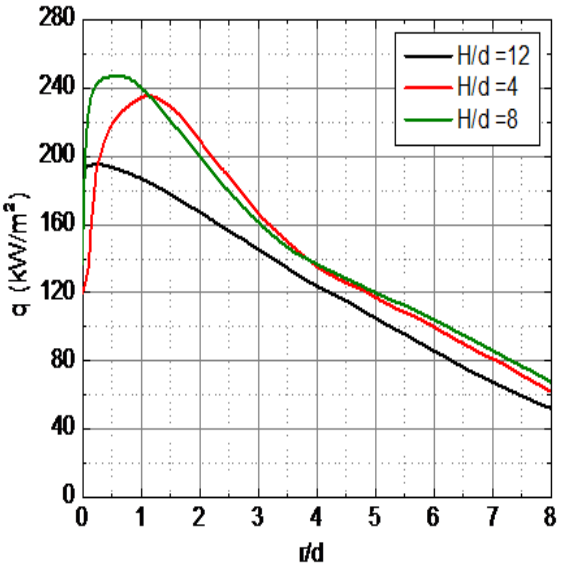

Fig. 8 Heat flux distributions for various plate separation distance (*Re* = 6000 and *ER* = 2)

It is evident from the fig. 6 and 7 that with increase in Reynolds number, the maximum heat flux increases for same *ER*. For *H/d* = 8 with *Re* = 6000, the maximum heat flux of

315.99 kW/m^2 occurs at a radial distance *r/d* = 0.49, whereas for *H/d* = 8 with *Re* = 10000, the maximum heat flux of 337.61 kW/m^2 occurs at a radial distance *r/d* = 0.69.

Similarly, the heat flux distributions at the plate surface for varius *H/d* for *ER* = 2, and fuel jet *Re* = 6000 is depicted in fig. 8. It can be seen from fig. 6, fig. 7 and fig. 8 that for *H/d* = 12, the maximum heat flux occurs very close to the center of the plate and as *H/d* decreases the maximum heat flux region gets shifted slightly away from the centre of the plate. For *Re* = 6000 and *ER* = 1, the maximum heat flux for *H/d* = 4 is 299.56 kW/m^2 and as *H/d* increases from 4 to 8, the maximum heat flux increases to 315.99 kW/m^2. Further increasing the *H/d* ratio from 8 to 12, the maximum heat flux decreases to 205.86 kW/m^2.

The gas phase temperature fields for diffusion flames for various *H/d* ratio are given in fig. 9, fig. 10 and fig. 11. The diffusion flame under this situation is lifted from the burner and becomes relatively thinner with more radial spread close to the plate surface as compared to the premixed flame (Tripathy et al. [10]). With increase in the value of *Re*, the flame region gets more attached to the plate surface with a relatively larger radial spread of the flame. This results in a higher heat fluxes at the plate surfaces. This may be due to the fact that the presence of the target plate spreads the flame in radial direction when the velocity of jet increases. For both *H/d* = 4 and 8, the flame appears to be plate stabilized annular flame with an un-reacted cool central core (Fig. 9 and 10). This core extends up to a distance very close to plate surface for *H/d* = 4. This results in a relatively high temperature zone in the stagnation region adjacent to the plate surface in case of *H/d* = 8. For *H/d* = 12, the flame appears like a nozzle stabilized envelop which gets deflected by the plate (Fig. 11). Under this situation, there exists a short un-reacted burner attached cool conical core which is surrounded by an umbrella like high temperature flame zone that extends almost up to the plate surface.

When *H/d* increases, the flame temperature decreases due to the entrainment of more air from the surrounding. The heat flux in stagnation region for *H/d* = 12 is relatively increased with the peak value being close to that for *H/d* = 8. This may be due to the fact that when Reynolds number increases the flame length also increases.

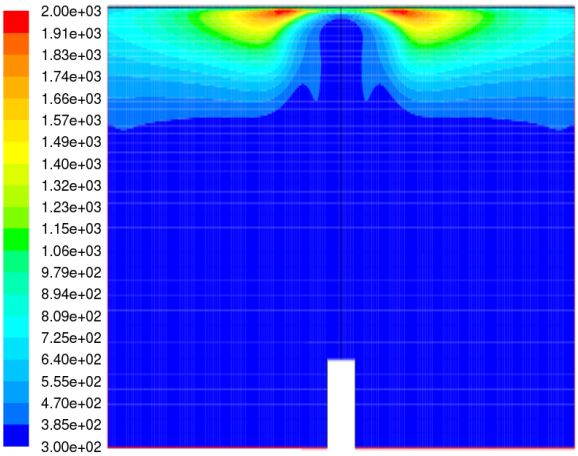

Fig. 9 Gas phase temperature fields for H/d = 4, ER = 1, and Re = 6000

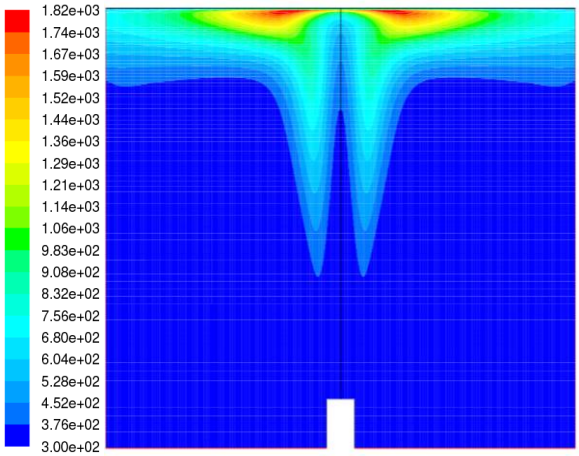

Fig. 10 Gas phase temperature fields for H/d = 8, ER = 1, and Re = 6000

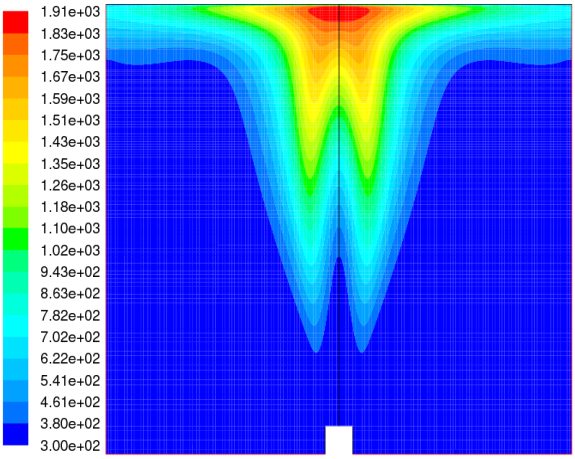

Fig. 11 Gas phase temperature fields for H/d = 12, ER = 1, and Re = 6000

Fig. 12 depicts the variations of average Nusselt number over the plate with *Re* for different values of plate separation distance. It can be observed from fig. 12 that average Nusselt number increases with increase in *Re*. The average Nusselt number $\bar{N}u$ also increases with decrease in the value of *H/d*. The increase in average Nusselt number is more pronounced for a change in H/d from 12 to 8 as compared to a change from 8 to 4 and that too in the higher range of Reynolds number. This can be attributed to the fact of having a more plate attached flame with lower values of *H/d* and at higher values of *Re*. Fig. 13 shows the dependence of average Nusselt number on Reynolds number for various equivalence ratio (*ER*) with *H/d* = 8. The equivalence ratio varies from 1.0 to 2.0. It is evident that when *ER* increases, average Nusselt number also increases. The increase in the value of $\bar{N}u$ with ER is more pronounced at higher values of Reynolds number (above *Re* = 6000). For a fuel rich mixture of ER=2 a favorable zone of burning is formed near thee plate due to entrainment o surrounding air, as a result of which the Nuselt number increases.

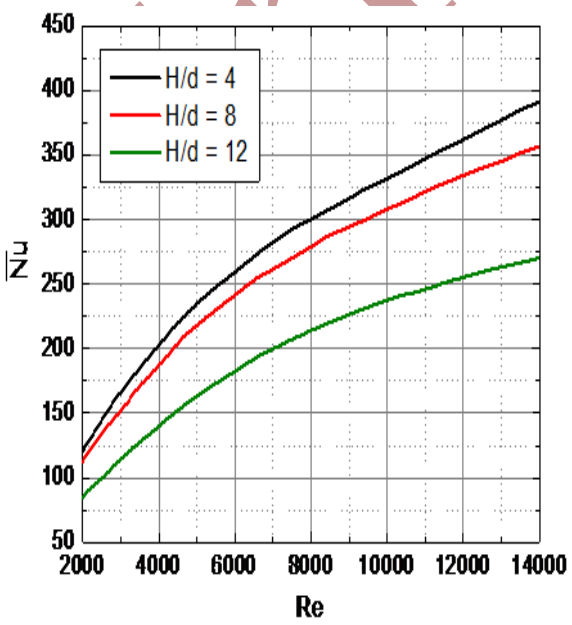

Fig. 12 Variations of average Nusselt number with *Re* for different values of *H/d* for *ER* = 1

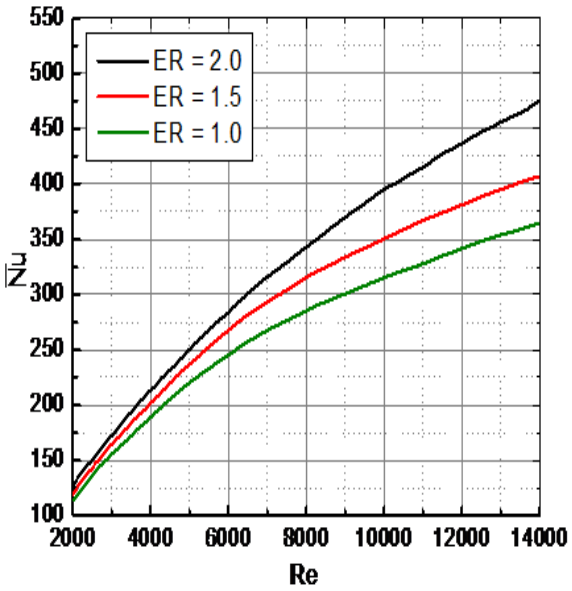

Fig. 13 Variations of average Nusselt number with *Re* for different values of *ER for H/d* = 8

5. Conclusions

Theoretical analysis of turbulent diffusion flames impinging normally on a plane surfaces have been developed to determine the average Nusselt number and the plate heat flux distribution as functions of jet Reynolds number, separation distance (H/d) and equivalence ratio (ER). The major observations made in this numerical study can be summarized as follows:

(i) The peak value of heat flux occurs at a location slight away from stagnation point and gradually decreases away from center of the plate.

(ii) The peak in the local heat flux comes closer to the stagnation point with an increase in the value of separation distance of the plate from the nozzle.

(iii) Heat flux gradually increases with decrease in the value of H/d from 12 to 8

but with further decrease in the value of H/d from 8 to 4, it decreases.

(iv) When Reynolds number increases, the average Nusselt number ($\bar{N}u$) increases for all values of separation distance and equivalence ratio.

(v) The average Nusselt number ($\bar{N}u$) also increases with an increase in Equivalence ratio (*ER*) for all values of plate separation distance and increase in the value of $\bar{N}u$ with *ER* is more prominent at higher values of Reynolds number (*Re*).

References

[1] C. E. Baukal, and B. Gebhart, "A review of empirical flame impingement heat transfer correlations", *Int. J. Heat Fluid Flow*, Vol. 17, pp.386-396, (1996).

[2] Y. E. Boke, O. Aydin and H. D. Yildizay, "The Comparison of Experimental and Predicted Flame Temperature of Natural Gas Combustion", *Energy Sources, Part A: Recovery, Utilization, and Environmental Effects*, Vol. 33, pp.1271-1280, (2011).

[3] S. Chander, and A. Ray, "Heat transfer characteristics of laminar methane/air flame impinging normal to a cylindrical surface", Experimental Thermal and Fluid Science, Vol. 32, pp.707-721 (2007).

[4] C. Cornaro, A.S. Fleischer, M. Rounds, and R. J. Goldstein, "Jet impingement cooling of convex semi-cylindrical surface", *International Journal of Thermal Science*, Vol. 40, pp. 890–898, (2001).

[5] L. L. Dong, C. S. Cheung, and C. W. Leung, "Heat transfer from an impinging premixed butane/air slot flame jet", *Int. J. Heat Mass Transfer*, Vol. 45, pp.979-992, (2002).

[6] S. S. Hou, and Y. C. Ko, "Influence of oblique angle and heating height on flame structure temperature field and efficiency of an impinging laminar jet flame", *Energy Conversion and Management*, Vol. 46, pp. 941–958, (2005).

[7] P. Kuntikana, and S. V. Prabhu, "Isothermal air jet and premixed flame jet pingement Heat transfer characterization and comparison", *International Journal of Thermal Sciences*, *Vol.* 100, pp. 401-415, (2016).

[8] G. K. Agrawal, S. Chakraborty, and S. K. Som, "Heat transfer characteristics of premixed flame impinging upwards to plane surfaces inclined with the flame jet axis". *International Journal of Heat and Mass Transfer*, Vol. 53, pp. 1899–1907, (2010).

[9] H. Lee, Y. S. Chung, and D. S. Kim, "Turbulent flow heat transfer measurement on curved surface with fully developed round impinging jet", *International Journal of Heat and Fluid Flow*, Vol. 18, pp.60–169, (1997).

[10] S. Tripathy, A. K. Rout, and M. K. Roul, "Heat Transfer due to Impinging Flame on Plane Surface", *International Organization of Scientific Research*, Vol. 13, pp. 27-34, (2016).

[11] A. Mirmohammadi, and F. Ommi, "Internal combustion engines in cylinder flow simulation improvement using nonlinear k-ε turbulence models", *Journal of Computational and Applied Research in Mechanical Engineering*, Vol. 5(1), pp. 61-69, (2015).

[12] S. Y. Ibrahim and O. D. Makinde, "Radiation effect on chemically reacting magneto hydrodynamics (MHD) boundary layer flow of heat and mass transfer through a porous vertical flat plate," Int. J. Physical Sciences, Vol. 6, No. 6, pp. 1508-1516, (2011).

[13] L. R. Reddy, M. C. Raju, G. S. S. Raju and S. M. Ibrahim, "Chemical reaction and thermal radiation effects on MHD micropolar fluid past a stretching sheet embedded in a non-Darcian porous medium", *Journal of Computational and Applied Research in Mechanical Engineering*, Vol. 6, No. 2, pp. 27-46, (2016).

[14] S. Mohammed Ibrahim and K. Suneetha, "Effects of thermal diffusion and chemical reaction on MHD transient free convection flow past a porous vertical plate with radiation, temperature gradient dependent

heat source in slip flow regime", *Journal of Computational and Applied Research in Mechanical Engineering*, Vol. 5, No. 2, pp. 83-95, (2015).

[15]J. Prakash, P. Durga Prasad, R. V. M. S. S. Kiran Kumar and S. V. K. Varma, "Diffusion-thermo effects on MHD free convective radiative and chemically reactive boundary layer flow through a porous medium over a vertical plate", *Journal of Computational and Applied Research in Mechanical Engineering*, Vol. 5, No. 2, pp. 111-126, (2015).

[16]M.J. Remie, M.F.G. Cremers, K.R.A.M. Schreel and L.P.H. de Goey, "Analysis of the heat transfer of an impinging laminar flame jet", *International Journal of Heat and Mass Transfer*, Vol. 50, pp. 2816-2827, (2007).

[17]M. Gnaneswara Reddy, and N. Sandeep, "Free convective heat and mass transfer of magnetic bio-convective flow caused by a rotating cone and plate in the presence of nonlinear thermal radiation and cross diffusion", *Journal of Computational and Applied Research in Mechanical Engineering*, Vol. 7, No. 1, pp. 1-21, (2017).

[18]Z. L. Wei, H. S. Zhen, C. W. Leung, C. S. Cheung and Z.H. Huang, "Heat transfer characteristics and the optimized heating distance of laminar premixed biogas hydrogen Bunsen flame impinging on a flat surface", *International Journal of Hydrogen Energy*, Vol. 40, pp. 15723-15731, (2015).

[19]G. Singh, S. Chander and A. Ray, "Heat transfer characteristics of natural gas/air swirling flame impinging on a flat surface", *Experimental Thermal and Fluid Science*, Vol. 41, pp. 165-176, (2012).

[20]R. C. Nayak, M. K. Roul, and S. K. Sarangi, "Experimental Investigation of Natural Convection Heat Transfer in Heated Vertical Tubes with Discrete Rings", *Experimental Techniques*, Vol. 41, pp. 585-603, (2017).

[21]R. C. Nayak, M. K. Roul, and S. K. Sarangi, "Natural Convection Heat Transfer in Heated Vertical Tubes with Internal Rings." *Archives of Thermodynamics*, Vol. 39(4), pp. 85-111, (2018)

[22]L. K. Sahoo, M. K. Roul, and R. K. Swain, "Natural convection heat transfer augmentation factor with square conductive pin fin arrays", *Journal of Applied Mechanics and Technical Physics*, Vol. 58, pp. 1115–1122, (2017).

[23]L. K. Sahoo, M. K. Roul, and R. K. Swain, "CFD Analysis of natural convection heat transfer augmentation from square conductive horizontal and inclined pin fin arrays", *International Journal of Ambient Energy*, Vol. 39, pp. 840-851, (2018)

[24]M. B. Gerdroodbary, M. Mokhtari, K. Fallah and H. Pourmirzaagha, "The influence of micro air jets on mixing augmentation of transverse hydrogen jet in supersonic flow", *International Journal of Hydrogen Energy*, Vol. 41 (47), pp.22497-22508, (2016).

[25]Y. Amini, M. Mokhtari, M. Haghshenasfard and M. B. Gerdroodbary, "Heat transfer of swirling impinging jets ejected from Nozzles with twisted tapes utilizing CFD technique", *Case Studies in Thermal Engineering*, Vol. 6, pp.104-115, (2015).

[26]M. B. Gerdroodbary, O. Jahanian and M. Mokhtari, "Influence of the angle of incident shock wave on mixing of transverse hydrogen micro-jets in supersonic crossflow", *International Journal of Hydrogen Energy*, Vol. 40, pp.9590-9601, (2015).

[27]M. B. Gerdroodbary, D.D. Ganji and Y. Amini, "Numerical study of shock wave interaction on transverse jets through multiport injector arrays in supersonic crossflow", *Acta Astronautica*, Vol. 115, pp.422-433, (2015).

[28]M. B. Gerdroodbary, M. Rahimi Takami and D.D. Ganji, "Investigation of thermal radiation on traditional Jeffery–Hamel flow to stretchable convergent/divergent channels", *Case Studies in Thermal Engineering*, Vol. 6, pp.28-39, (2015).

[29]K. Fallah, M. B. Gerdroodbary, A. Ghaderi and J. Alinejad, "The influence of

micro air jets on mixing augmentation of fuel in cavity flame holder at supersonic flow", *Aerospace Science and Technology*, Vol. 76, pp.187-193, (2018).

[30]B. E. Poling J. M. Prausnitz and J. P. O'Connell, *The Properties of Gases and Liquids*, 5th ed., McGraw Hill Book Company, New York, (2001).

[31]B. F. Magnussen, and B. H. Hjertager, "On mathematical modelling of turbulent combustion with specified emphasis on soot formation and combustion", *The combustion institute Cambridge* USA, Vol. 16, pp. 719-729, (1977).

[32]T. H. Vander Meer, "Stagnation point heat transfer from turbulent low Reynolds number jets and flame jets". *Expt. Thermal Fluid Sci.* Vol. 4, pp. 115-126, (1991).